Free-energy functional for freezing transitions: Hard-sphere systems freezing into crystalline and amorphous structures

Swarn Lata Singh, Atul S. Bharadwaj, and Yashwant Singh
Department of Physics, Banaras Hindu University, Varanasi 221 005, India
(Received 31 January 2011; published 23 May 2011)

A free-energy functional that contains both the symmetry-conserved and symmetry-broken parts of the direct pair correlation function has been used to investigate the freezing of a system of hard spheres into crystalline and amorphous structures. The freezing parameters for fluid-crystal transition have been found to be in very good agreement with the results found from simulations. We considered amorphous structures found from molecular dynamics simulations at packing fractions η lower than the glass close packing fraction η_J and investigated their stability compared to that of a homogeneous fluid. The existence of a free-energy minimum corresponding to a density distribution of overlapping Gaussians centered around an amorphous lattice depicts a deeply supercooled state with a heterogeneous density profile.

DOI: 10.1103/PhysRevE.83.051506 PACS number(s): 64.70.D−, 05.70.Fh, 64.70.pm

I. INTRODUCTION

When a liquid freezes into a crystalline solid its continuous symmetry of translation and rotation is broken into one of the Bravais lattices. In three dimensions the freezing of a liquid into a crystalline solid is known to be a first-order symmetry-breaking transition marked by large discontinuities in entropy, density, and order parameters. The molecules in a crystal are localized on a lattice described by a discrete set of vectors $\{\mathbf{R}_i\}$ such that any functions of position, such as one-particle density $\rho(\mathbf{r})$, satisfies $\rho(\mathbf{r}) = \rho(\mathbf{r} + \mathbf{R}_i)$ for all $\mathbf{R}_i$ [1]. This set of vectors necessarily forms a Bravais lattice. But when a liquid is supercooled bypassing its crystallization, it continues to remain in an amorphous state. With increase in density a solidlike phase emerges with molecules getting localized around their mean positions, which have a random structure. The underlying lattice on which such localized motion takes place is related to the time scale of relaxation in the supercooled liquid. While the supercooled liquid starts to attain solidlike properties, structurally it does not have any long-range order like the one present in a crystal. This phenomenon is termed the "glass transition" [2,3]. Although glassy materials are well characterized experimentally, the existence of a thermodynamic phase transition into the glassy state remains controversial [4–6]. Our aim in this paper is not to enter into this discussion but to examine the stability (or metastability) of amorphous structures from a thermodynamic point of view, using the standard method of density-functional theory, which is also used to investigate the crystallization of liquids. We refer to a structure in which particles are localized around their mean positions forming a random lattice as a glassy or an amorphous solid. Localization of particles amounts to breaking of continuous translational symmetry of the normal liquid and takes place in forming both crystals and glasses.

The structural properties of a classical system can be adequately described by one- and two-particle density distributions. The equilibrium one-particle density distribution $\rho(\mathbf{r})$ defined as

$$\rho(\mathbf{r}) = \left\langle \sum_k \delta(\mathbf{r} - \mathbf{R}_k) \right\rangle, \tag{1.1}$$

where $\mathbf{R}_k$ is the position vector of the kth particle and bracket $\langle \cdots \rangle$ represents the ensemble average, is a constant independent of position for an isotropic liquid, but contains most of the information about the structure of crystals and glasses. The two-particle density distribution $\rho^{(2)}(\mathbf{r}_1,\mathbf{r}_2)$, which gives the probability of finding simultaneously a molecule in a volume element $d\mathbf{r}_1$ centered at $\mathbf{r}_1$ and a second molecule in volume element $d\mathbf{r}_2$ centered at $\mathbf{r}_2$, is defined as

$$\rho^{(2)}(\mathbf{r}_1,\mathbf{r}_2) = \left\langle \sum_j \sum_{\neq k} \delta(\mathbf{r}_1 - \mathbf{R}_j)\delta(\mathbf{r}_2 - \mathbf{R}_k) \right\rangle. \tag{1.2}$$

The pair correlation function $g(\mathbf{r}_1,\mathbf{r}_2)$ is related to $\rho^{(2)}(\mathbf{r}_1,\mathbf{r}_2)$ by the relation

$$g(\mathbf{r}_1,\mathbf{r}_2) = \frac{\rho^{(2)}(\mathbf{r}_1,\mathbf{r}_2)}{\rho(\mathbf{r}_1)\rho(\mathbf{r}_2)}. \tag{1.3}$$

The direct pair correlation function $c(\mathbf{r}_1,\mathbf{r}_2)$, which appears in the expression of free-energy functional (see Sec. II), is related to the total pair correlation function $h(\mathbf{r}_1,\mathbf{r}_2) = g(\mathbf{r}_1,\mathbf{r}_2) - 1$ through the Ornstein-Zernike (OZ) equation:

$$h(\mathbf{r}_1,\mathbf{r}_2) = c(\mathbf{r}_1,\mathbf{r}_2) + \int c(\mathbf{r}_1,\mathbf{r}_3)\rho(\mathbf{r}_3)h(\mathbf{r}_2,\mathbf{r}_3)\,d\mathbf{r}_3. \tag{1.4}$$

Since in an isotropic liquid $\rho(\mathbf{r}_1) = \rho(\mathbf{r}_2) = \rho_l = N/V$ where N is the average number of molecules in volume V,

$$g(|\mathbf{r}_2 - \mathbf{r}_1|) = \frac{\rho^{(2)}(|\mathbf{r}_2 - \mathbf{r}_1|)}{\rho_l^2}, \tag{1.5}$$

where $|\mathbf{r}_2 - \mathbf{r}_1| = r$ is the magnitude of interparticle separation. In a liquid of spherically symmetric particles $g(\mathbf{r}_1,\mathbf{r}_2)$, $h(\mathbf{r}_1,\mathbf{r}_2)$, $c(\mathbf{r}_1,\mathbf{r}_2)$ depend only on the interparticle separation r. This simplification is due to homogeneity, which implies continuous translational symmetry, and isotropy, which implies continuous rotational symmetry. Such simplification does not, in general, occur for frozen phases. We refer to crystals as well as to glasses as frozen phases. While a crystal is both inhomogeneous and anisotropic, a glass can be regarded as isotropic but inhomogeneous. The heterogeneity in a glassy system over different length and time scales has been studied in recent work [7] related to computer simulations.

The total and direct pair correlation functions of a system can be obtained as a simultaneous solution of the OZ equation and a closure relation that relates pair correlation functions to the pair potential. Some well-known closure relations are the Percus-Yevick (PY) relation, the hypernetted chain (HNC) relation, and the mean spherical approximation (MSA). It may, however, be noted that while the OZ equation (1.4) is general and connects the total and direct pair correlation functions of liquids as well as of frozen phases, the closure relations have been derived assuming translational invariance [8] and therefore are valid only for normal fluids. The integral equation theory has been used quite successfully to describe the structure of isotropic liquids, but its application to frozen phases has so far been very limited [9,10]. In Sec. III we describe a method to calculate the direct pair correlation function of frozen phases formed by breaking of continuous translational symmetry of liquids and use it in a free-energy functional described in Sec. II to study freezing transitions in Secs. IV and V.

Since its proposal in 1979 by Ramakrishnan and Yussouff (RY) [11], density functional theory (DFT) has been applied to the freezing transition of a variety of pure liquids and mixtures [11,12]. A DFT requires an expression of the Helmholtz free energy (or the grand thermodynamic potential) in terms of one- and two-particle distribution functions and a relation that relates $\rho(\mathbf{r})$ to pair correlation functions. Such a relation is found by minimizing the free energy with respect to $\rho(\mathbf{r})$ with appropriate constraints [12,13]. The DPCFs that appear in these equations are in the frozen phase and are functionals of $\rho(\mathbf{r})$. When this functional dependence is ignored and the DPCF is replaced by that of the coexisting isotropic liquid [11] or by that of an "effective homogeneous fluid" [14] the free-energy functional becomes approximate and fails to provide an accurate description of freezing transitions and stability of frozen phases. An improved free-energy functional that takes into account the functional dependence of the DPCF on $\rho(\mathbf{r})$ has recently been developed [9,10] and applied to study the isotropic-nematic transition [9] and the crystallization of power-law fluids [10].

In this paper we investigate the freezing of fluids of hard spheres into crystalline and amorphous phases and compare our results with the results of previous investigations. Hard spheres are ubiquitous in condensed matter; they have been used as models of liquids, crystals, colloidal systems, granular systems, and powders. Packing of hard spheres is of even wider interest as they are related to important problems in information theory, such as signal digitalization, error correcting codes, and optimization problems [15]. Recently, amorphous packing of hard spheres has attracted much attention [6,16,18] because for polydisperse colloids and granular materials the crystalline state is not obtained for kinetic reasons. It is therefore necessary to have a statistical-mechanical theory based on first principles that can correctly describe the freezing of hard spheres.

The paper is organized as follows: In Sec. II we describe the free-energy functional for a symmetry-broken phase that contains both the symmetry-conserving and symmetry-broken parts of direct pair correlation functions. In Sec. III we describe a method to calculate these correlation functions. The theory is applied in Sec. IV to investigate the freezing of fluids into crystalline solids and in Sec. V the metastability of amorphous structures.

II. FREE-ENERGY FUNCTIONAL

An important step in the construction of a density functional model of a frozen phase is the proper parametrization of the extremely inhomogeneous density function $\rho(\mathbf{r})$ whose value near a lattice site may be orders of magnitude higher than in the interstitial regions. One very successful prescription of $\rho(\mathbf{r})$ is as a collection of overlapping Gaussian profiles [19] centered over a set of lattice sites $\{\mathbf{R}_m\}$:

$$\rho(\mathbf{r}) = \sum_m \left(\frac{\alpha}{\pi}\right)^{3/2} \exp[-\alpha(\mathbf{r}-\mathbf{R}_m)^2]. \tag{2.1}$$

Here α is the variational parameter that characterizes the width of the Gaussian; the square root of α is inversely proportional to the width of the peaks. It thus measures the nonuniformity; the value $\alpha = 0$ corresponds to the limit of a uniform liquid (infinitely broad Gaussians), and an increasing value of α corresponds to increasing localization of the atoms about their respective lattice sites.

Taking the Fourier transform of (2.1) one gets

$$\rho(\mathbf{r}) = \rho_0 + \frac{1}{V}\sum_{q\neq 0} \rho_q e^{i\mathbf{q}\cdot\mathbf{r}}, \tag{2.2}$$

where

$$\rho_q = e^{-q^2/4\alpha} \sum_n e^{-i\mathbf{q}\cdot\mathbf{R}_n} \tag{2.3}$$

is the amplitude of a density wave of wavelength $2\pi/|q|$. The nature and magnitude of inhomogeneity of a frozen phase is measured by ρ_q, hereafter referred to as the order parameter; $\rho_q = 0$ for $q \neq 0$ corresponds to isotropic fluid and $\rho_q \neq 0$ to a frozen phase. For a crystal in which $\mathbf{R}_m$ forms a periodic lattice, $e^{i\mathbf{q}\cdot\mathbf{R}_m} = \delta_{\mathbf{q},\mathbf{G}}$ where $\mathbf{G}$ are reciprocal lattice vectors (RLVs), Eq. (2.2) reduces to

$$\rho_s(\mathbf{r}) = \rho_0 + \rho_0 \sum_G e^{-G^2/4\alpha} e^{i\mathbf{G}\cdot\mathbf{r}}. \tag{2.4}$$

This is a well-known expression for $\rho(\mathbf{r})$ of a crystal.

In the case of a glassy structure in which the lattice sites $\{R_m\}$ are randomly distributed, the summation in Eq. (2.3) is replaced by integration. For this, one uses the value of site-site correlation function $g(R)$ as the number of lattice sites located in a spherical shell of width dR, and radius R is given as $4\pi\rho_0 g(R)R^2 dR$. Thus for an amorphous structure Eq. (2.1) reduces to

$$\rho_g(r) = \rho_0 + \frac{1}{V}\sum_{q\neq 0} e^{-q^2/4\alpha}\left\{1 + \rho_0\left[\int d\mathbf{R} h(R) e^{-i\mathbf{q}\cdot\mathbf{R}}\right]\right\} e^{i\mathbf{q}\cdot\mathbf{r}}, \tag{2.5}$$

where $g(R) = 1 + h(R)$. The value of $g(R)$ is found either from experiment on glassy systems [20] or from numerical simulations [21,22]. In Fig. 1 we plot $\rho_g(r)$ for the packing fraction η ($\equiv \frac{1}{6}\pi\rho_0\sigma^3$; σ being the diameter of a particle) = 0.576 and $\alpha = 150$ (highly localized condition) and $\alpha = 15$ (weakly localized condition). The distance r in this and in the subsequent figures is expressed in units of σ. In calculating

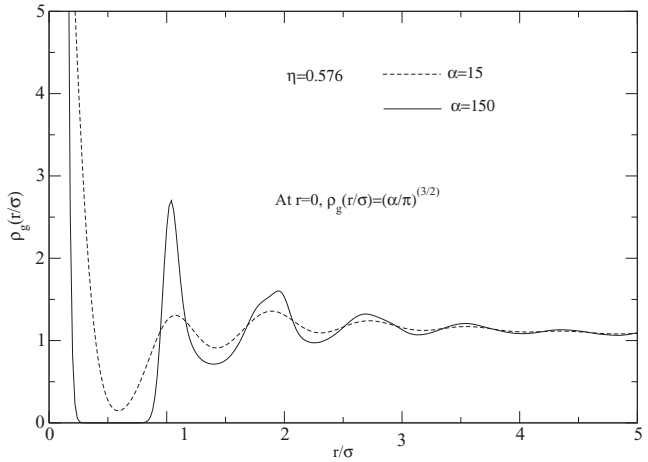

FIG. 1. Density $\rho_g(\frac{r}{\sigma})$ of an amorphous structure calculated from Eq. (2.5) using the data of $g\left(\frac{R}{\sigma}\right)$ found from molecular dynamic simulation of granular particles subjected to a sequence of vertical tapes for $\alpha = 150$ (strong localization condition) and $\alpha = 15$ (weak localization condition).

$\rho_g(r)$ we used $g(R)$ data found for amorphous structures of granular particles [22] shown in Fig. 2. In Fig. 2 we also show the value of $g(R)$ of a liquid found from solving the integral equations discussed in Sec. III, for comparison. From Fig. 1 we see that while inhomogeneity increases with the value of α, unlike crystalline solids, it remains confined to about four particle diameters even for $\alpha = 150$ and decays rapidly on increasing the distance.

The reduced free energy $A[\rho]$ of an inhomogeneous system is a functional of $\rho(\mathbf{r})$ and is written as

$$A[\rho] = A_{id}[\rho] + A_{ex}[\rho]. \tag{2.6}$$

The ideal gas part is exactly known and is given as

$$A_{id}[\rho] = \int d\mathbf{r}\rho(\mathbf{r})\{\ln[\rho(\mathbf{r})\Lambda] - 1\}, \tag{2.7}$$

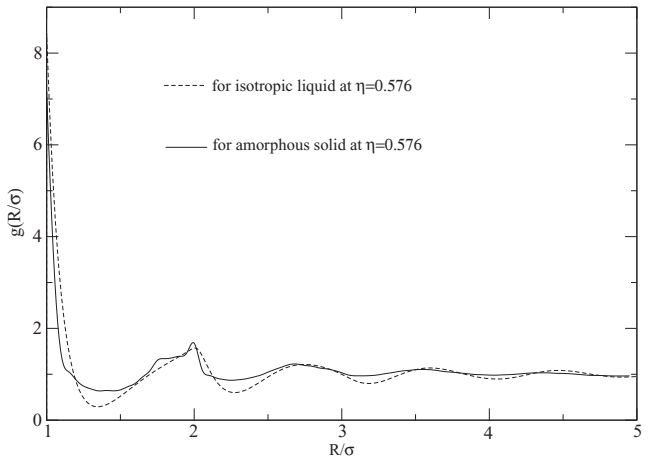

FIG. 2. Comparison of pair correlation function $g\left(\frac{R}{\sigma}\right)$ of an amorphous structure and homogeneous liquid at the same packing fraction $\eta = 0.576$.

where Λ is a cube of the thermal wavelength associated with a molecule. The excess part arising due to intermolecular interactions is related to the DPCF as [12]

$$\frac{\delta^2 A_{ex}[\rho]}{\delta\rho(\mathbf{r}_1)\delta\rho(\mathbf{r}_2)} = -c(\mathbf{r}_1,\mathbf{r}_2;[\rho]). \tag{2.8}$$

The function c that appears in this equation is the functional of $\rho(\mathbf{r})$ and can be written as a sum of two terms: one that corresponds to the average density ρ_0 and is found by treating the system to be homogeneous and isotropic, and the other that arises due to the heterogeneity in the density of the frozen phase. Thus

$$c(\mathbf{r}_1,\mathbf{r}_2,[\rho]) = c^{(0)}(|\mathbf{r}_2 - \mathbf{r}_1|,\rho_0) + c^{(b)}(\mathbf{r}_1,\mathbf{r}_2;[\rho]). \tag{2.9}$$

Note that while $c^{(0)}$ depends on the magnitude of the interparticle separation and is a function of the average number density ρ_0, $c^{(b)}$ is invariant only under a discrete set of translations corresponding to lattice vectors $\{R_m\}$ and is a functional of $\rho(\mathbf{r})$. It may be noted that at the freezing point the homogeneity of the space is spontaneously broken and, as a consequence, the correlation in distribution of molecules loses the translational invariance of the fluid phase. This change of symmetry leads to writing the distribution functions of a frozen phase as a sum of two qualitatively different contributions [9,10]. This for the case of the single-particle distribution $\rho(\mathbf{r})$ has already been shown. In Eq. (2.4) for a crystalline solid and in Eq. (2.5) for an amorphous solid, $\rho(\mathbf{r})$ is shown to have two contributions: one that corresponds to continuous symmetry and the other to the broken symmetry. Similarly in Eq. (2.9) while $c^{(0)}$ corresponds to the symmetry-conserving part, $c^{(b)}$ corresponds to the symmetry-broken part of the DPCF. While $c^{(0)}$ passes smoothly without any abrupt change through transition, $c^{(b)}$ vanishes in the fluid phase.

Using Eq. (2.9) we rewrite Eq. (2.8) as

$$\frac{\delta^2 A_{\rm ex}^{(0)}[\rho]}{\delta\rho(\mathbf{r}_1)\delta\rho(\mathbf{r}_2)} = -c^{(0)}(r,\rho_0), \tag{2.10}$$

$$\frac{\delta^2 A_{\rm ex}^{(b)}[\rho]}{\delta\rho(\mathbf{r}_1)\delta\rho(\mathbf{r}_2)} = -c^{(b)}(\mathbf{r}_1,\mathbf{r}_2;[\rho]), \tag{2.11}$$

where $A_{\rm ex}^{(0)}[\rho] + A_{\rm ex}^{(b)}[\rho] = A_{ex}[\rho]$. $A_{\rm ex}^{(0)}$ and $A_{\rm ex}^{(b)}$ are found from functional integrations of (2.10) and (2.11), respectively. In this integration the system is taken from some initial density to the final density $\rho(\mathbf{r})$ along a path in the density space; the result is independent of the path of integration. As the symmetry-conserving part $c^{(0)}$ is function of density only, the integration of Eq. (2.10) in the density space is done taking an isotropic fluid of density ρ_0 (or ρ_l, the density of coexisting fluid in case of a crystal) as a reference. This leads to

$$A_{\rm ex}^{(0)}[\rho] = A_{\rm ex}(\rho_0) - \frac{1}{2}\int d\mathbf{r}_1 \int d\mathbf{r}_2 \Delta\rho(\mathbf{r}_1)\Delta\rho(\mathbf{r}_2)c^{(0)}(r,\rho_0), \tag{2.12}$$

where $\Delta\rho(\mathbf{r}_1) = \rho(\mathbf{r}_1) - \rho_0$ and $A_{\rm ex}(\rho_0)$ is the excess reduced free energy of an isotropic system of density ρ_0.

In order to do functional integration of Eq. (2.11) in which $c^{(b)}[\rho]$ depends on order parameters in addition to the average density, we chose a path in density space that is characterized by two parameters, λ and ξ. These parameters vary from 0 to 1. The parameter λ raises the average density from 0 to the

final value ρ_0 as it varies from 0 to 1, whereas the parameter ξ raises the order parameters from 0 to their final value ρ_q for each q as it varies from 0 to 1. The integration gives [9,10]

$$A_{ex}^{(b)}[\rho] = -\frac{1}{2}\int d\mathbf{r}_1 \int d\mathbf{r}_2 \Delta\rho(\mathbf{r}_1)\Delta\rho(\mathbf{r}_2)\bar{c}^{(b)}(\mathbf{r}_1,\mathbf{r}_2;[\rho]), \tag{2.13}$$

where

$$\bar{c}^{(b)}(\mathbf{r}_1,\mathbf{r}_2;[\rho]) = 4\int_0^1 d\xi\xi \int_0^1 d\xi' \int_0^1 d\lambda\lambda \times \int_0^1 d\lambda' c^{(b)}(\mathbf{r}_1,\mathbf{r}_2;\lambda\lambda'\rho_0;\xi\xi'\rho_q). \tag{2.14}$$

While integrating over λ the order parameter ρ_q are kept fixed, and while integrating over ξ the density is kept fixed. The result does not depend on the order of integration. The free-energy functional of a frozen phase is the sum of $A_{id}[\rho]$, $\Delta A^{(0)}[\rho]$, and $\Delta A^{(b)}[\rho]$ given, respectively, by Eqs. (2.7),(2.12), and (2.13).

The minimization of $\Delta A[\rho] = A[\rho] - A(\rho_0)$ where $A(\rho_0)$ is the free energy of a homogeneous and isotropic system of density ρ_0 leads to

$$\ln\frac{\rho(\mathbf{r})}{\rho_0} = \phi + \int d\mathbf{r}_2 \Delta\rho(\mathbf{r}_2)c^{(0)}(|\mathbf{r}_2-\mathbf{r}_1|,\rho_0) + \int d\mathbf{r}_2 \Delta\rho(\mathbf{r}_2)\bar{c}^{(b)}(\mathbf{r}_1,\mathbf{r}_2). \tag{2.15}$$

Here ϕ is the Lagrange multiplier and is determined from the condition

$$\frac{1}{V}\int_V \frac{\rho(r)}{\rho_0} d\mathbf{r} = 1 \tag{2.16}$$

and

$$\tilde{c}^{(b)}(\mathbf{r}_1,\mathbf{r}_2) = 2\int_0^1 d\lambda \int_0^1 d\xi c^{(b)}(\mathbf{r}_1,\mathbf{r}_2,\lambda\rho_0,\xi\rho_q). \tag{2.17}$$

In principle, the only information we need to know is the value of $c^{(0)}(r)$ and $c^{(b)}(\mathbf{r}_1,\mathbf{r}_2;[\rho])$ to calculate self-consistently the value of $\rho(\mathbf{r})$ that minimizes the free energy. In practice, one, however, finds it convenient to do minimization for an assumed form of $\rho(\mathbf{r})$ [12].

III. CALCULATION OF DIRECT PAIR CORRELATION FUNCTION

To calculate the values of $c^{(0)}(r)$ we use the integral equation theory consisting of the OZ equation:

$$h^{(0)}(r) = c^{(0)}(r) + \rho_0 \int d\mathbf{r}' c^{(0)}(r')h^{(0)}(|\mathbf{r}'-\mathbf{r}|) \tag{3.1}$$

and a closure relation proposed by Rogers and Young [23]. This closure relation is written as

$$1 + h^{(0)}(r) = \exp[-u(r)/k_BT]\left\{1 + \frac{\exp[\gamma(r)f(r)]-1}{f(r)}\right\}, \tag{3.2}$$

where

$$\gamma(r) = h(r) - c(r) \tag{3.3}$$

and

$$f(r) = 1 - \exp(-\psi r). \tag{3.4}$$

Here ψ is an adjustable parameter used to achieve thermodynamic consistency, and its value for a system of hard spheres is found to be equal to 0.16 [23]. In Eq. (3.2) $u(r)$ is the pair potential, k_B the Boltzmann constant, and T temperature. This closure relation was found by mixing the PY and HNC closure relations in such a way that at $r = 0$ it reduces to the PY approximation, and for values of r where $f(r)$ approaches 1, it reduces to the HNC approximation. Equations (3.1)–(3.4) together constitute a thermodynamically consistent theory that has been found to give values of pair correlation functions that are in very good agreement with Monte Carlo results.

The differentiation of Eqs. (3.1) and (3.2) with respect to density yields the following two relations:

$$\frac{\partial h^{(0)(r)}}{\partial\rho_0} = \frac{\partial c^{(0)}(r)}{\partial\rho_0} + \int d\mathbf{r}' c^{(0)}(r')h^0(|\mathbf{r}'-\mathbf{r}|) + \rho_0\int d\mathbf{r}'\frac{\partial c^{(0)}(r)}{\partial\rho_0}h^{(0)}(|\mathbf{r}'-\mathbf{r}|) + \rho_0\int d\mathbf{r}' c^{(0)}(r)\frac{\partial h^{(0)}(|\mathbf{r}'-\mathbf{r}|)}{\partial\rho_0} \tag{3.5}$$

and

$$\frac{\partial h^{(0)}(r)}{\partial\rho_0} = \exp\left[-\frac{u(r)}{k_BT}\right]\left\{\exp[\gamma(r)f(r)]\frac{\partial\gamma(r)}{\partial\rho_0}\right\}. \tag{3.6}$$

The closed set of coupled equations (3.1), (3.2), (3.5), and (3.6) have been solved using Gillen's algorithm [24] for four unknowns: $h^{(0)}$, $c^{(0)}$, $\frac{\partial h^{(0)}}{\partial\rho_0}$, and $\frac{\partial c^{(0)}}{\partial\rho_0}$. We compare the values of $c^{(0)}(r)$ at packing fractions $\eta = 0.50$ and 0.55 in Fig. 3 and values of $\frac{\partial c^{(0)}(r)}{\partial\rho_0}$ for the same two values of η in Fig. 4 to see the density dependence of these functions. While $\eta = 0.50$ is close to the value of packing fraction at which a system freezes into a crystalline solid, $\eta = 0.55$ is close to the value of packing fraction η_M at which the crystal melts.

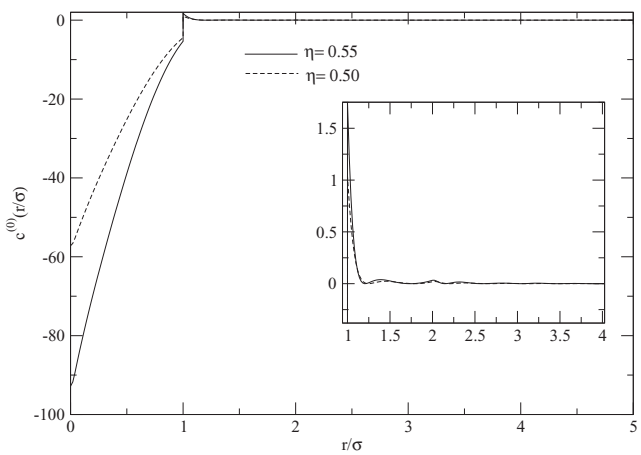

FIG. 3. Direct pair correlation function $c^{(0)}(\frac{r}{\sigma})$ as a function of distance $\frac{r}{\sigma}$ at packing fraction $\eta = 0.50$ and 0.55 found from the integral equation theory. The inset shows at magnified scale the value for $\frac{r}{\sigma} \geqslant 1$.

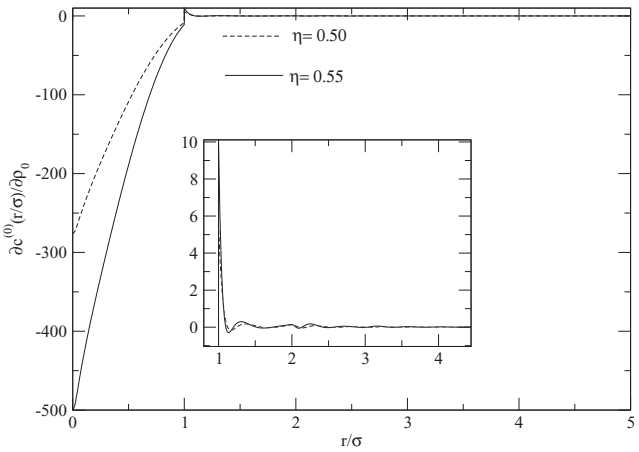

FIG. 4. Density derivatives of direct pair correlation function $c^{(0)}(\frac{r}{\sigma})$ at $\eta = 0.50$ and 0.55 found from the integral equation theory. The inset shows at magnified scale the value for $\frac{r}{\sigma} \geqslant 1$.

Since all closure relations [including the one given by Eq. (3.2)] that are used in the integral equation theory for pair correlation functions are derived assuming translational invariance [8], their use in calculating the values of pair correlation functions of frozen phases may not be correct. In view of this we use a series expansion in which the contribution to the DPCF arising due to inhomogeneity in density of the system is expressed in terms of higher-body direct correlation functions of the uniform (isotropic and homogeneous) system. Thus [12],

$$c^{(b)}(\mathbf{r}_1,\mathbf{r}_2;[\rho]) = \int d\mathbf{r}_3 c_3^{(0)}(\mathbf{r}_1,\mathbf{r}_2,\mathbf{r}_3;\rho_0)[\rho(\mathbf{r}_3)-\rho_0] + \int d\mathbf{r}_3 d\mathbf{r}_4 c_4^{(0)}(\mathbf{r}_1,\mathbf{r}_2,\mathbf{r}_3,\mathbf{r}_4)[\rho(\mathbf{r}_3) - \rho_0][\rho(\mathbf{r}_4)-\rho_0] + \cdots, \tag{3.7}$$

where $\rho(\mathbf{r}_n) - \rho_0 = \sum_{q\neq 0} \rho_q e^{i\mathbf{q}\cdot\mathbf{r}_n}$. In Eq. (3.7) $c_n^{(0)}$ are N-body direct correlation functions of the uniform system. These correlation functions can be found using the relations

$$\frac{\delta c^{(0)}(r)}{\delta\rho_0} = \int d\mathbf{r}_3 c_3^{(0)}(\mathbf{r}_1,\mathbf{r}_2,\mathbf{r}_3), \tag{3.8}$$

$$\frac{\delta^2 c^{(0)}(r)}{\delta\rho_0^2} = \int d\mathbf{r}_3 d\mathbf{r}_4 c_4^{(0)}(\mathbf{r}_1,\mathbf{r}_2,\mathbf{r}_3,\mathbf{r}_4), \tag{3.9}$$

etc. The values of derivatives of $c^{(0)}(r)$ appearing on the left-hand side of the above equations have been found using the integral equation theory described above.

We note that Eq. (3.7) satisfies the condition that $c^{(b)}$ is zero in the fluid phase and depends on the magnitudes (order parameters) and the phase factors of density waves. These density waves measure the nature and magnitude of inhomogeneity of frozen phases. While each wave contributes independently to the first term of Eq. (3.7), interactions between the two waves contribute to the second term, and so on. The contributions made by successive terms of Eq. (3.7) depend on the range of pair potential $u(r)$ [10]. As the range of potential increases, the contribution made by higher-order terms increases. For a system of hard spheres we find that at the freezing transition the contribution made by the first term to free energy is already small, and therefore higher-order terms are expected to be negligible; it is only for $u(r) \propto r^{-n}$, $n < 12$ that the contribution made by the second-order term becomes important [10]. In view of fast convergence of the series, Eq. (3.7) seems to be a useful expression for calculating $c^{(b)}(\mathbf{r}_1,\mathbf{r}_2)$.

The first term of Eq. (3.7) involves a three-body direct correlation function, which can be factorized as a product of two-body functions [25]. Thus

$$c_3^{(0)}(\mathbf{r}_1,\mathbf{r}_2,\mathbf{r}_3;\rho_0) = t(r_{12})t(r_{13})t(r_{23}). \tag{3.10}$$

The function $t(r)$ is determined using the relation of Eq. (3.8):

$$\frac{\partial c^{(0)}(r)}{\partial\rho_0} = t(r)\int d\mathbf{r}' t(r')t(|\mathbf{r}'-\mathbf{r}|). \tag{3.11}$$

We adopt the numerical procedure developed in Ref. [25] to calculate $t(r)$ from known values of $\frac{\delta c^{(0)}(r)}{\delta\rho_0}$ from (3.11). The values of $t(r)$ are plotted in Fig. 5 for $\eta = 0.50$ and 0.55 to show their density dependence.

Taking only the first term of Eq. (3.7) we write

$$c^{(b)}(\mathbf{r}_1,\mathbf{r}_2) = \frac{1}{V}\sum_q\sum_n \mu_q \int d\mathbf{r}_3 t(|\mathbf{r}_3-\mathbf{r}_1|) \times e^{i\mathbf{q}(\mathbf{r}_3-\mathbf{R}_n)} t(|\mathbf{r}_3-\mathbf{r}_2|), \tag{3.12}$$

where $\mu_q = e^{-q^2/4\alpha}$ Using the relation

$$\mathbf{r}_3 = \tfrac{1}{2}(\mathbf{r}_1+\mathbf{r}_2) - \tfrac{1}{2}(\mathbf{r}_2-\mathbf{r}_1) + (\mathbf{r}_3-\mathbf{r}_1), \tag{3.13}$$

we find that $c^{(b)}(\mathbf{r}_1,\mathbf{r}_2)$ can be written in a Fourier series in the center-of-mass variable $\mathbf{r}_c = \frac{1}{2}|\mathbf{r}_1+\mathbf{r}_2|$ with coefficients that are a function of the difference variable $\mathbf{r} = \mathbf{r}_2 - \mathbf{r}_1$, i.e.,

$$c^{(b)}(\mathbf{r}_1,\mathbf{r}_2) = \frac{1}{V}\sum_q c^{(q)}(\mathbf{r}) e^{i\mathbf{q}\cdot\mathbf{r}_c}, \tag{3.14}$$

where

$$c^{(q)}(\mathbf{r}) = \sum_n \mu_q e^{-i\mathbf{q}\cdot\mathbf{R}_n} e^{-\frac{1}{2}i\mathbf{q}\cdot\mathbf{r}} \int d\mathbf{r}' t(r') e^{i\mathbf{q}\cdot\mathbf{r}'} t(|\mathbf{r}'-\mathbf{r}|). \tag{3.15}$$

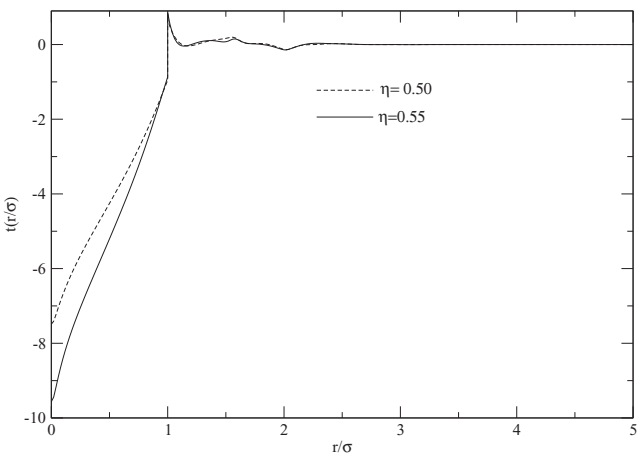

FIG. 5. Values of $t(\frac{r}{\sigma})$ as a function of distance for $\eta = 0.50$ and 0.55.

Since the DPCF is real and symmetric with respect to the interchange of $\mathbf{r}_1$ and $\mathbf{r}_2$, $c^{(q)}(\mathbf{r}) = c^{(-q)}(\mathbf{r})$ and $c^{(q)}(\mathbf{r}) = c^{(q)}(-\mathbf{r})$. For given values of α and $\mathbf{R_n}$ one can calculate $c^{(q)}(r)$ from known values of $t(r)$. We discuss our results for crystalline and amorphous solids in the following sections.

IV. CRYSTALLINE SOLID

A. Calculation of $c^{(b)}(\mathbf{r_1},\mathbf{r_2})$

For a crystal in which vectors $\mathbf{R}_n$ form a Bravais lattice, Eqs. (3.14) and (3.15) can be written as [10]

$$c^{(b)}(\mathbf{r}_1,\mathbf{r}_2) = \sum_G c^{(G)}(\mathbf{r}) e^{i\mathbf{G}\cdot\mathbf{r}_c} \tag{4.1}$$

and

$$c^{(G)}(\mathbf{r}) = \rho_0 \mu_G e^{-\frac{1}{2}i\mathbf{G}\cdot\mathbf{r}} \int d\mathbf{r}' t(r') e^{i\mathbf{G}\cdot\mathbf{r}'} t(|\mathbf{r}' - \mathbf{r}|), \tag{4.2}$$

where $\mu_G = e^{-G^2/4\alpha}$. Equation (4.2) has been solved using the Rayleigh expansion to give

$$c^{(G)}(\mathbf{r}) = \sum_{lm} c_{lm}^{(G)}(r) Y_{lm}(\hat{r}), \tag{4.3}$$

where

$$c_{lm}^{(G)}(r) = \frac{\rho_0 \mu_G}{2\pi^2} \sum_{l_1}\sum_{l_2} (i)^{l_1+l_2}(-1)^{l_2}\left[\frac{(2l_1+1)(2l_2+1)}{2l+1}\right] \times [C_g(l_1,l_2,l;0,0,0)]^2 j_{l_2}\left(\frac{1}{2}Gr\right) t(r) B_{l_1}(r,G) Y_{lm}^*(\hat{G}). \tag{4.4}$$

Here C_g is the Clebsch-Gordan coefficient, $j_l(x)$ the spherical Bessel function, and

$$B_{l_1}(r,G) = (4\pi)^2 \int dk k^2 t(k) j_{l_1}(kr) \times \int dr' r'^2 t(r') j_{l_1}(kr') j_{l_1}(Gr'). \tag{4.5}$$

The crystal symmetry dictates that l and $l_1 + l_2$ are even and for a cubic crystal, $m = 0, \pm 4$. Here $c_{lm}^{(G)}(r)$ depends on the order parameter and on the magnitude of RLVs.

The Fourier transform of $c^{(G)}(\mathbf{r})$ defined as

$$c^{(G)}(\mathbf{k}) = \int c^{(G)}(\mathbf{r}) e^{-i\mathbf{k}\cdot\mathbf{r}} d\mathbf{r} = \sum_{lm} c_{lm}^{(G)}(k) Y_{lm}(\hat{k}), \tag{4.6}$$

where

$$c_{lm}^{(G)}(k) = 4\pi (i)^l \int dr r^2 j_l(kr) c_{lm}^{(G)}(r) \tag{4.7}$$

is calculated from the knowledge of $c_{lm}^{(G)}(r)$. In Fig. 6 we plot $c_{lm}^{(G)}(k)$ for the first two sets of G at $\eta = 0.55$ and $\alpha = 170$ for a face-centered cubic (FCC) structure.

B. Liquid-solid transition

The grand thermodynamic potential defined as $-W = A - \beta\mu \int d\mathbf{r}\rho(\mathbf{r})$, where μ is the chemical potential, is used to locate the transition as it ensures that the pressure and chemical potentials of the two phases remain equal at the transition.

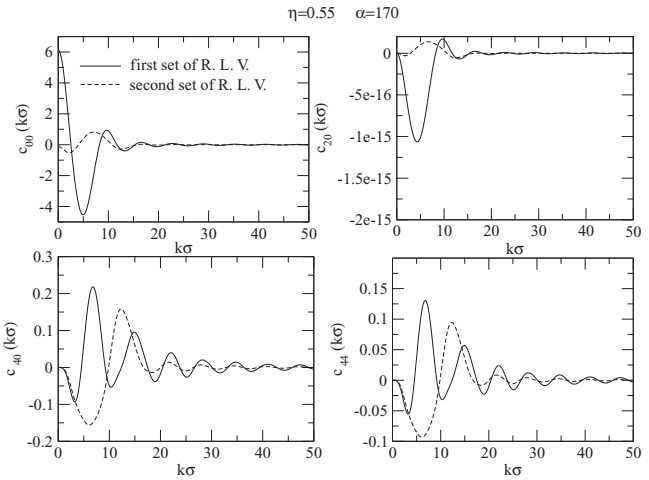

FIG. 6. Values of harmonic coefficients $c^{(G)}{}_{lm}(k\sigma)$ for the first two sets of reciprocal lattice vectors of a FCC crystal for $\eta = 0.55$ and $\alpha = 170$.

The transition point is determined by the condition $\Delta W = W_l - W = 0$, where W_l is the grand thermodynamic potential of the fluid. Using expressions given in Sec. II we find

$$\frac{\Delta W}{N} = \frac{\Delta W_{\rm id}}{N} + \frac{\Delta W_0}{N} + \frac{\Delta W_b}{N}, \tag{4.8}$$

where

$$\frac{\Delta W_{\rm id}}{N} = 1 - \ln\rho_l + (1+\Delta\rho^*)\left[\frac{3}{2}\ln\left(\frac{\alpha}{\pi}\right) - \frac{5}{2}\right], \tag{4.9}$$

$$\frac{\Delta W}{N} = -\frac{1}{2}\Delta\rho^{*2}\hat{c}^{(0)}(0) - \frac{1}{2}\sum_{G\neq 0}(1+\Delta\rho^*)^2 |\mu_G|^2 \hat{c}^{(0)}(\mathbf{G}), \tag{4.10}$$

$$\frac{\Delta W_b}{N} = -\frac{1}{2}\sum_{G_1}{}' \sum_{G}{}' (1+\Delta\rho*)^2 \mu_G \mu_{-G-G_1} \hat{\bar{c}}^{(G)} \times \left(\mathbf{G}_1 + \frac{1}{2}\mathbf{G}\right). \tag{4.11}$$

Here $\Delta W_{\rm id}$, ΔW_0, and ΔW_b are, respectively, the ideal, symmetry-conserving, and symmetry-broken contributions to ΔW; the prime on summations in Eq. (4.11) indicates the condition, $\mathbf{G} \neq 0$, $\mathbf{G}_1 \neq 0$, and $\mathbf{G} + \mathbf{G}_1 \neq 0$, and

$$\hat{c}^{(0)}(\mathbf{G}) = \rho_l \int c^{(0)}(r) e^{i\mathbf{G}\cdot\mathbf{r}} d\mathbf{r}, \tag{4.12}$$

$$\hat{\bar{c}}\left(\mathbf{G}_1 + \frac{1}{2}\mathbf{G}\right) = \rho_0 \sum_{lm} \int \bar{c}_{lm}^G(r,\rho_0) e^{i(\mathbf{G}_1 + \frac{1}{2}\mathbf{G})\cdot\mathbf{r}} Y_{lm}(\hat{r}) d\mathbf{r}, \tag{4.13}$$

where $\rho_0 = \rho_l(1+\Delta\rho^*)$.

We used the above expression to locate the fluid-FCC solid and fluid-body-centered cubic (BCC) solid transitions by varying the values of ρ_l, $\Delta\rho^*$, and α. While we find the fluid-FCC solid transition to take place at $\eta_l = 0.490$, $\Delta\eta^* = 0.106$, and $\alpha = 170$, no transition is found for a BCC solid. In Table I we compare our results of freezing parameters with those found by Monte Carlo simulation [26,27] and from other density functional schemes [28–31]. The agreement

TABLE I. Freezing parameters of a hard-sphere fluid derived from the various density functional schemes. Here $L = \left(\frac{3}{\alpha}\right)^{1/2}\left(\frac{3\eta_s}{2\pi}\right)^{1/3}$ is the Lindemann parameter, $\eta_s = \frac{\pi}{6}\rho_s\sigma^3$, $\eta_l = \frac{\pi}{6}\rho_l\sigma^3$, and $\Delta\eta^* = \frac{\eta_s - \eta_l}{\eta_l}$. Average errors are given in parentheses. MWDA stands for modified weighted density approximation; RY DFT stands for Ramakrishnan-Yussouff density functional theory.

	η_s	η_l	$\Delta\eta^*$	L
Present result	0.542 (<1%)	0.490(<1%)	0.106(<1%)	0.09
MWDA-static reference [27]	0.503(8%)	0.452(8%)	0.115(10%)	0.13
MWDA [28]	0.548(<1%)	0.474(4%)	0.156(49%)	0.10
RY DFT [29,30]	0.60(10%)	0.511(3%)	0.174(69%)	0.06
Simulation [25,26]	0.545	0.493	0.105	∼0.13

found between our results and those of simulations are very good, better than any other density functional schemes.

At the transition point the contribution of different terms of Eq. (4.8) is as follows: $\frac{\Delta W_{id}}{N} = 4.44$, $\frac{\Delta W_0}{N} = -4.10$, $\frac{\Delta W_b}{N} = -0.34$. The contribution made by the symmetry-breaking term of free energy is about 8.3% to that of the symmetry-conserving term. This is in accordance with the result found earlier [10] for the inverse power potential $u(r) = \epsilon(\sigma/r)^n$, where ϵ, σ, and n are potential parameters, that as n increases ($n = \infty$ corresponds to hard-sphere potential) the contribution made by the symmetry-breaking term to free energy decreases. This explains why RY theory [11], while it gave good results for the hard-spheres system, failed for potentials that have soft repulsion and/or attractive tails.

V. AMORPHOUS STRUCTURE

In this section we investigate the heterogeneous density profile of an amorphous structure and examine the question of having metastable states between the normal fluid state and the regular crystalline state at packing fraction η, which lies between the packing fraction at the melting point of a crystal $\eta_M = 0.545$ and the packing fraction corresponding to the "glass close packing," $\eta_J \simeq= 0.65$. The usual way to construct an amorphous structure in experiment or in numerical simulation is to compress the system according to some protocol that avoids crystallization [17,21,22]. One of the criteria used to signal the onset of the glassy phase in supercooled liquids is the emergence of a split-second peak in $g(R)$. There may be an infinitely large number of such metastable structures that when compressed jam along a continuous finite range densities down to the glass close packing η_J [32,33].

The density functional approach provides the means to test if such a structure is stable compared to that of a fluid at a given temperature and density. In earlier calculations the random close-packed structure generated through Bennett's algorithm [34] was used. Here $g(R)$ giving the distribution of particles at a given value of η was found using an *ad hoc* scaling relation [35]:

$$g(R) = g_B\left[R\left(\frac{\eta}{\eta_J}\right)^{1/3}\right], \tag{5.1}$$

where η_J was used as a scaling parameter such that at $\eta = \eta_J$ the random close-packed structure $g_B(R)$ was obtained. While Singh *et al.* [36] found that the state corresponding to this structure becomes more stable than the fluid for $\eta \geqslant 0.59$ for a very large value of α (~ 280), which corresponds to a highly inhomogeneous density distribution, Kaur and Das [37] found that the same structure also becomes more stable than fluid for $\eta \geqslant 0.576$ for a considerably smaller value of α ($\simeq 18$). On the other hand, Dasgupta [38] has numerically located the "glassy" minimum of a free-energy functional and the structure that gave this minimum. Here we use the value of $g(R)$ found for granular particles from molecular dynamics simulations [22] at $\eta = 0.576$ and 0.596 and examine the stability of these structures. The reason for choosing these data is that they are available for $\eta < \eta_J$ and can, therefore, be used directly in the theory without using any approximation such as relation (5.1).

A. Calculation of $c^{(b)}(\mathbf{r}_1, \mathbf{r}_2)$

From the known values of $g(R)$ the order parameter defined by Eq. (2.3) is calculated. Thus, for $q \neq 0$

$$\rho_q = \sum_n e^{-q^2/4\alpha} e^{-i\mathbf{q}\cdot\mathbf{R}_n} = \mu_q S_a(q), \tag{5.2}$$

where $\mu_q = e^{-q^2/4\alpha}$ and $S_q(a) = 1 + 24\eta \int dR R^2 (g(R) - 1)\, j_0(qR)$. In Fig. 7 we plot ρ_q as a function of q for $\alpha = 15$ and 50 and $\eta = 0.596$. The values of the order parameters μ_G for several **G** of an FCC crystal for $\alpha = 50$ and $\eta = 0.596$ are also shown for comparison. From the figure one may note that the value of ρ_q of an amorphous structure has a very different

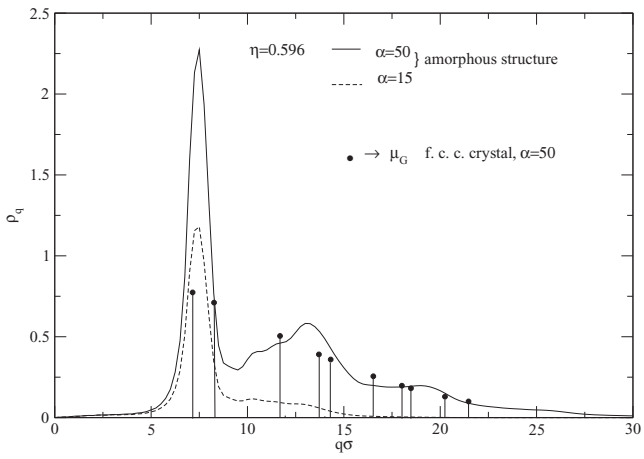

FIG. 7. Comparison of order parameters of amorphous structure for $\alpha = 50$ and 15 and of a FCC crystal for $\alpha = 50$ (up to 10th neighbors) at $\eta = 0.596$.

magnitude and dependence on wave vector **q** than that of a crystal.

Using the fact that an amorphous structure can be considered on average to be isotropic, Eq. (3.15) is simplified to give

$$c^{(q)}(r) = \frac{1}{8\pi^3}\mu_q S_a(q)t(r)\sum_q (2l+1)B_l(q,r)j_l\left(\frac{1}{2}qr\right), \tag{5.3}$$

where

$$B_l(q,r) = (4\pi)^2 \int dk k^2 t(k) j_l(kr) \int dr' r'^2 t(r') j_l(kr') j_l(qr'). \tag{5.4}$$

In Fig. 8 we show the value of $c^{(q)}(r)$ as a function of r for q at which $\mu_q S_a(q)$ is maximum for $\alpha = 15$ and $\eta = 0.596$.

B. Determination of free-energy minimum

We calculate the minimum of $\Delta A[\rho] = A[\rho] - A_l(\rho_0)$, where $A_l(\rho_0)$ is the reduced free energy of an isotropic fluid of density ρ_0 and $A[\rho]$ is the reduced free energy of an amorphous structure of average density ρ_0. Using the expression given in Sec. II we get

$$\frac{\Delta A[\rho]}{N} = \frac{\Delta A_{id}[\rho]}{N} + \frac{\Delta A_0[\rho]}{N} + \frac{\Delta A_b[\rho]}{N}, \tag{5.5}$$

$$\frac{\Delta A_{id}[\rho]}{N} = 4\pi\left(\frac{\alpha}{\pi}\right)^{3/2}\int dr r^2 e^{-\alpha r^2} \ln\left\{\left[\left(\frac{\alpha}{\pi}\right)^{3/2} e^{-\alpha r^2}\right] + \frac{\rho_0}{r}\left(\frac{\alpha}{\pi}\right)^{1/2}\int dR R g(R) \times (e^{-\alpha(r-R)^2} - e^{-\alpha(r+R)^2})\right\} - \ln\rho_0 \tag{5.6}$$

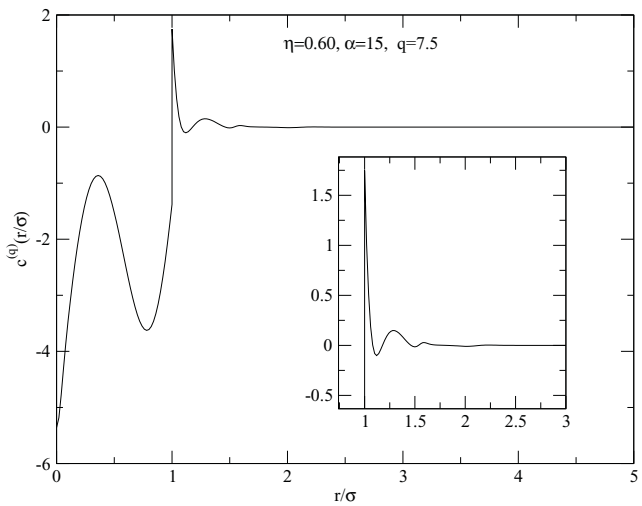

FIG. 8. Values of $c^{(q)}(\frac{r}{\sigma})$ as a function of distance $\frac{r}{\sigma}$ at $q = 7.53$ at which ρ_q is maximum. Inset magnifies the value of $c^{(q)}(\frac{r}{\sigma})$ for $\frac{r}{\sigma} \geqslant 1$.

for $\alpha < 20$,

$$\frac{\Delta A_{id}[\rho]}{N} = 1 - \ln\rho_0 + \frac{3}{2}\left[\ln\left(\frac{\alpha}{\pi}\right) - \frac{5}{3}\right] \tag{5.7}$$

for $\alpha > 20$,

$$\frac{\Delta A_0[\rho]}{N} = -\frac{1}{2}\sum_q |\mu_q|^2 S_a(q)\hat{c}^{(0)}(q), \tag{5.8}$$

$$\frac{\Delta A_b[\rho]}{N} = -\frac{1}{2}\sum_q\sum_{q_1}\mu_{q_1}\mu_{-q-q_1}S_a(q_1)\hat{\bar{c}}^{(q)}\left(\left|\mathbf{q}_1 + \frac{1}{2}\mathbf{q}\right|\right), \tag{5.9}$$

where

$$\hat{\bar{c}}^{(q)}\left(\mathbf{q}_1 + \frac{1}{2}\mathbf{q}\right) = \int \bar{c}^{(q)}(r) e^{i\left(\mathbf{q}_1 + \frac{1}{2}\mathbf{q}\right)\cdot\mathbf{r}} d\mathbf{r}$$

and

$$\bar{c}^{(q)}(r) = 4\int d\lambda\lambda \int d\lambda' \int d\xi\xi \int d\xi' c^{(q)}(r,\lambda\lambda'\rho_0,\xi\xi'\rho_q).$$

In Fig. 9 we plot the values of ΔA found for different values of α. A minimum of ΔA is found at $\alpha \simeq 7$ for both $\eta = 0.576$ and 0.596. This minimum is seen only for the amorphous structure, which signifies a heterogeneous density distribution and is referred to as glassy minimum. From the figure it is clear that the glassy minimum is separated from the liquid minimum by a barrier located at $\alpha \simeq 0.6$; the height of the barrier increases with the density. The value of α corresponding to the minimum is inversely proportional to the root mean square displacement of the particles from their sites. Since $\frac{1}{\sqrt{(\alpha)}} = 0.37$, this is a case of weak localization as the root-mean-square displacement is about five times larger than that of the crystal ($\frac{1}{\sqrt{\alpha}} = 0.08$) at the freezing point. Therefore this free-energy minimum can be associated with a deeply supercooled state [39,40] with density distribution of overlapping Gaussians centered around an amorphous lattice.

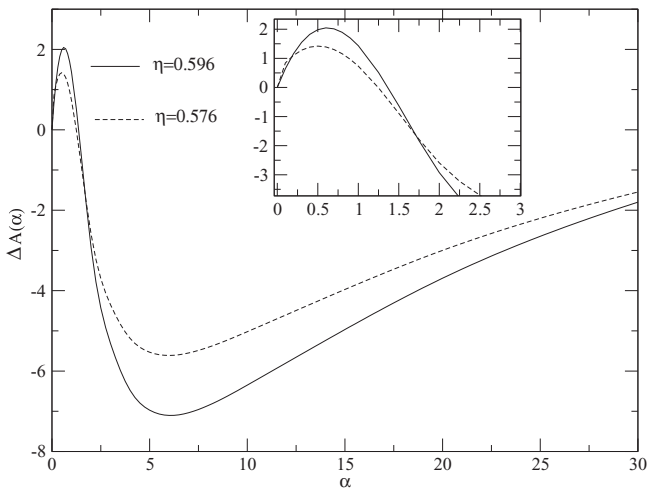

FIG. 9. Free-energy difference $\Delta A = A[\rho_0] - A_l[\rho_0]$ as a function of localization parameter α at $\eta = 0.576$ and 0.596 for amorphous structures. The inset shows at magnified scale the energy barrier that separates the minimum of amorphous structure from that of homogeneous fluid.

The schematic phase diagram that one expects in the presence of a glass transition contains a pressure line that bifurcates from that of the liquid at some $\eta > \eta_b$ and that diverges at η_J [6]. The bifurcation point is connected with the onset of glass transition. The pressure of a system can be found from the knowledge of single- and two-particle density distributions. For example, the virial pressure of a system in three dimensions is given as

$$\frac{\beta P}{\rho_0} = 1 - \frac{1}{6k_B T N} \int d\mathbf{r}_1 \times \int d\mathbf{r}_2 \rho(\mathbf{r}_1)\rho(\mathbf{r}_2) g(\mathbf{r}_1,\mathbf{r}_2)[\mathbf{r}\cdot\nabla\mathbf{u}(\mathbf{r})], \quad (5.10)$$

where $\mathbf{r} = \mathbf{r}_2 - \mathbf{r}_1$. For an amorphous structure of hard spheres this reduces to

$$\frac{\beta P}{\rho_0} = 1 + \frac{2}{3}\pi\rho_0 g(1) + \frac{2\pi}{3} g(1) \sum_{q\neq 0} |\mu_q|^2 S_a(q) j_0(q). \quad (5.11)$$

Note that for an isotropic fluid the third term of the above equation is zero; the bifurcation of the pressure line from that of the normal fluid starts as soon as particles start getting localized. Localization of particles also leads to crossover from nonactivated to activated dynamics and considerable increase in relaxation time.

VI. SUMMARY AND PERSPECTIVES

A free-energy functional that contains both the symmetry-conserved part of the DPCF $c^{(0)}(r)$ and the symmetry-broken part $c^{(b)}(\mathbf{r}_1,\mathbf{r}_2)$ has been used to investigate the freezing of a system of hard spheres into crystalline and amorphous structures. The values of $c^{(0)}(r)$ and its derivatives with respect to density ρ_0 as a function of distance r have been found using integral equation theory comprising the OZ equation and a closure relation proposed by Roger and Young [23]. For $c^{(b)}(\mathbf{r}_1,\mathbf{r}_2)$ we used an expansion in ascending powers of order parameters. This expansion involves higher-body direct correlation functions of the isotropic phase, which in turn were found from the density derivatives of $c^{(0)}(r)$. For this we used the ansatz [25] embodied in Eqs. (3.10) and (3.11). The contribution made by the symmetry-broken term to the free energy at the freezing point (liquid-crystal transition point) was found to be about 8% of the symmetry-conserving part. Though this contribution is small, but, as shown in Table I it improves the agreement between theoretical values of the freezing parameters and the values found from simulations. This result and the results reported earlier [10] for the power-law fluids show that the contribution of the symmetry-broken part of the free energy increases with the softness of the potential. This explains why the RY free-energy functional was found to give a reasonably good description of the freezing transition of hard-spheres fluid but failed for potentials that have soft core and/or attractive tail. These results also indicate that the theory described here can be used to describe the freezing transitions of all kinds of potentials.

We used the free-energy functional to investigate the question of having metastable states between the homogeneous liquid and the regular crystalline state. The value of the site-site correlation function $g(R)$ that provides the structural description of the amorphous structure has been taken from a molecular dynamics simulation of a granular system subjected to a sequence of vertical taps [22]. The system has been found to behave like a glass-forming system. The reason for our choosing these data is that they are available for $\eta < \eta_J$ [22] and therefore can be used directly in the theory without using approximations such as scaling relation (5.1). Using the data of $g(R)$ at $\eta = 0.576$ and 0.596 from Ref. [22] we examined the stability of amorphous structures with respect to the homogeneous fluid. The minimum of free energy found at $\alpha \simeq 7$ suggests that the structures are stable compared to that of the fluid and corresponds to a density distribution of overlapping Gaussians centered around an amorphous lattice. This kind of structure may be associated with deeply supercooled states with a heterogeneous density profile. The transition of the liquid into any of these states will be determined by considering the dynamics of fluctuations around these minima. The glassy minimum is separated from the homogeneous liquid minimum by an energy barrier that height increases with the density.

Among future applications, it will be instructive to investigate the contribution made by the second term of Eq. (3.7) to free energy of different potentials, application of the theory to the freezing transition in two dimensions, in particular to examine the melting through the hexatic phase that other density functional schemes have failed to show, and the possibility of calculating total pair correlation functions of frozen phases using the OZ equation.

ACKNOWLEDGMENTS

We are thankful to Massimo Pica Ciamarra and A. Donev for providing the data of $g(R)$ and to T. V. Ramakrishnan for stimulating discussions. S.L.S. thanks the University Grants Commission for support.

[1] P. M. Chaikin and T. C. Lubensky, *Principles of Condensed Matter Physics* (Cambridge University Press, Cambridge, 1995).
[2] M. D. Ediger, C. A. Angell, and S. Nagel, J. Phys. Chem. **100**, 13200 (1996).
[3] P. G. Debenedetti and F. H. Stillinger, Nature (London) **410**, 259 (2001).
[4] L. O. Hedges, R. L. Jack, J. P. Garrahan, and D. Chandler, Science **323**, 1309 (2009).
[5] A. Cavagna, Phys. Rep. **476**, 51 (2009).
[6] G. Parisi and F. Zamponi, Rev. Mod. Phys. **82**, 789 (2010).
[7] W. Kob, C. Donati, S. J. Plimpton, P. H. Poole, and S. C. Glotzer, Phys. Rev. Lett. **79**, 2827 (1997).
[8] J. P. Hensen and I. R. Mc Donald, *Theory of Simple Liquids*, 3rd ed. (Academic press, Boston, 2006).
[9] P. Mishra and Y. Singh, Phys. Rev. Lett. **97**, 177801 (2006).
[10] S. L. Singh and Y. Singh, Europhys. Lett. **88**, 16005 (2009).

[11] T. V. Ramakrishnan and M. Yussouff, Phys. Rev. B **19**, 2775 (1979).
[12] Y. Singh, Phys. Rep. **207**, 351 (1991).
[13] H. Lowen, Phys. Rep. **237**, 249 (1994).
[14] A. R. Denton and N. W. Ashcroft, Phys. Rev. A **39**, 4701 (1989); A. Klein and N. W. Ashcroft, Phys. Rev. Lett. **78**, 3346 (1997).
[15] J. H. Conway and N. J. A. Sloane, *Sphere Packings, Lattices and Groups* (Springer-Verlag, New York, 1993).
[16] S. Torquato, T. M. Truskett, and P. G. Debenedetti, Phys. Rev. Lett. **84**, 2064 (2000).
[17] C. S. O'Hern, S. A. Langer, A. J. Liu, and S. R. Nagel, Phys. Rev. Lett. **88**, 075507 (2002); L. E. Silbert, A. J. Liu, and S. R. Nagel, Phys. Rev. E **73**, 041304 (2006).
[18] R. D. Kamien and A. J. Liu, Phys. Rev. Lett. **99**, 155501 (2007).
[19] P. Tarazona, Mol. Phys. **52**, 81 (1984).
[20] R. Zallen, *The Physics of Amorphous Solids* (John Wiley and Sons, New York, 1998).
[21] A. Donev, F. H. Stilinger, and S. Torquato, Phys. Rev. Lett. **96**, 225502 (2006); A. Donev, R. Connelly, F. H. Stillinger, and S. Torquato, Phys. Rev. E **75**, 051304 (2007).
[22] M. Pica Ciamarra, M. Nicodemi, and A. Coniglio, Phys. Rev. E **75**, 021303 (2007).
[23] F. J. Rogers and D. A. Young, Phys. Rev. A **30**, 999 (1984).
[24] M. J. Gillan, Mol. Phys. **38**, 1781 (1979).
[25] J. L. Barrat, J. P. Hansen, and G. Pastore, Mol. Phys. **63**, 747 (1988); Phys. Rev. Lett. **58**, 2075 (1987).
[26] W. G. Hoover and F. H. Ree, J. Chem. Phys. **49**, 3609 (1968).
[27] B. J. Alder, W. G. Hoover, and D. A. Young, J. Chem. Phys. **49**, 3688 (1968).
[28] D. C. Wang and A. P. Gast, J. Chem. Phys. **110**, 2522 (1999).
[29] B. B. Laird and D. M. Kroll, Phys. Rev. A **42**, 4810 (1990).
[30] J. L. Barrat, J. P. Hansen, G. Pastore, and E. M. Waisman, J. Chem. Phys. **86**, 6360 (1987).
[31] B. B. Laird, J. D. McCoy, and A. D. J. Heymat, J. Chem. Phys. **87**, 5449 (1987).
[32] L. Berthier and T. A. Witten, Phys. Rev. E **80**, 021502 (2009); Y. Burmer and D. R. Reichman, *ibid.* **69**, 041202 (2004).
[33] P. Chaudhuri, L. Berthier, and S. Sastry, Phys. Rev. Lett. **104**, 165701 (2010).
[34] C. Bennet, J. Appl. Phys. **43**, 2727 (1972).
[35] M. Baus and Jean-Louis Colot, J. Phys. C **19**, L135 (1986); H. Lowen, J. Phys. Condens. Matter **2**, 8477 (1990).
[36] Y. Singh, J. P. Stoessel, and P. G. Wolynes, Phys. Rev. Lett. **54**, 1059 (1985).
[37] C. Kaur and S. P. Das, Phys. Rev. Lett. **86**, 2062 (2001).
[38] C. Dasgupta, Europhys. Lett. **20**, 131 (1992); C. Dasgupta and O. T. Valls, Phys. Rev. E **59**, 3123 (1999).
[39] F. H. Stillinger, Science **267**, 1935 (1995).
[40] R. A. La Violette and F. H. Stillinger, J. Chem. Phys. **83**, 4079 (1985).